

Chapter 2

Coupled Schrödinger equations for two-body collisions

This chapter presents the two-body scattering theory of cold ground state alkali atoms. Section 2.1 begins with the coupled Schrödinger equations that describe the two-body collision dynamics. In addition, the appropriate scattering boundary conditions applied to these coupled differential equations are discussed. Physical observables of primary interest include scattering cross sections, event rates, and scattering lengths which are derived in subsections 2.1.1 and 2.1.2. In particular, the identical particle aspects of scattering by spin-dependent potentials are handled in detail. Section 2.2 discusses the physical interactions included in the coupled Schrödinger equations. These are the Born-Oppenheimer potentials (subsection 2.2.1), the atomic hyperfine Hamiltonian (subsection 2.2.2), the magnetic dipole-dipole interaction (subsection 2.2.3), and the effects of an external magnetic field (subsection 2.2.4). The coupled Schrödinger equations can be solved in any of several different angular momentum representations. Those of greatest importance are discussed in section 2.3. Subsection 2.3.1 develops the symmetrization of each representation while subsection 2.3.2 presents the unitary transformations between representations.

2.1 Scattering theory

Quantum two-body scattering theory is a well established subject presented in numerous textbooks (see for example, Ref.[24, 25]). However, scattering of identical particles with spin is still a tricky subject which can often lead to factor of two errors if one is not careful. I begin by briefly deriving a very general form of the coupled Schrödinger equations. The most general form of boundary conditions applied here is given in terms of a scattering amplitude $f(\theta, \phi)$. Subsection 2.1.1 relates the symmetrized scattering amplitude $f(\theta, \phi) + f(\pi - \theta, \pi + \phi)$ to the scattering cross section and to the event rate. While these relationships are derived within the Born approximation, they should have applicability to nonperturbative processes. At the end of this subsection, the physical observables are still given in terms of the Born integrals over the potential. These integrals are related to

symmetrized scattering \underline{S} and transition \underline{T} matrices in subsection 2.1.2. In particular, the four spin permutations of identical particle scattering for both isotropic and anisotropic potentials are examined carefully, tracking all factors of two. The final relationships among the cross sections, event rates, and scattering lengths in terms of the symmetrized \underline{S} - and \underline{T} -matrix elements are given in this subsection.

The forces on an atom in a trap depend, to a good approximation, only on the atom's position in the trap and not explicitly on time. The time independent Schrödinger equation

$$H\Psi = E\Psi \quad (2.1)$$

is therefore a proper starting point to describe the collision physics. A standard approach for solving two-body collision problems is to separate the center-of-mass motion from the relative motion of the atoms. This step is valid provided the forces on the two colliding atoms (labeled a and b) depend only on their relative orientation $\vec{R} = \vec{r}_a - \vec{r}_b$ and not their absolute position. Separating coordinates sounds a little counterintuitive since the goal of this theory is to describe **trapped** atoms. The “degree” of coordinate separability can be established by considering the relevant length scales in our problem. First, the range of a cold scattering event is roughly $R \leq 10^3$ Bohr. Typical magnetic trapping fields can be described accurately by an anisotropic harmonic potential which in the center-of-mass coordinate system is given by $V = \frac{1}{2}\mu(\omega_x x^2 + \omega_y y^2 + \omega_z z^2)$. Here $R^2 = x^2 + y^2 + z^2$, μ is the reduced mass of the pair, and ω the angular frequency of the trapping field. A pure quadratic field is still separable as is evident from the coordinate dependence in V . It is only the presence of anharmonic terms (e.g., $V \propto R^3$) which would couple the center-of-mass and relative motions. However, these anharmonicities are several orders of magnitude smaller than the quadratic potential. Considering the isotropic case and plugging in typical values for ^{87}Rb collisions ($\omega \sim 100$ Hz), the harmonic trapping potential adds an additional $1\mu\text{K}$ of energy only when the internuclear separation is larger than $R \sim 3(10^6)$ a.u., well beyond the distance one needs to consider for collisions. The trapping fields can therefore be safely neglected, which permits the center-of-mass motion to be removed from the scattering problem.

A multicomponent wave function representing the relative motion of the particles can be written in spherical coordinates as

$$\Psi = R^{-1} \sum_{lmk} F_{lmk}(R) Y_{lm}(\theta, \phi) \chi_k . \quad (2.2)$$

Here, the angular degrees of freedom are represented by an expansion in spherical harmonics Y_{lm} . (This is the partial wave expansion treated in textbooks). The spin degrees of freedom are labeled χ_k and $F_{lmk}(R)$ represents a set of radial functions to be determined. Insertion of this form for Ψ into Eq. 2.1 and projection onto $Y_{l'm'} \chi_{k'}$

leads to an infinite set of coupled differential equations of the form ($\Phi_i \equiv Y_{lm}\chi_k$)

$$\sum_f \left[\delta_{fi} \left(-\frac{1}{2\mu} \frac{\partial^2}{\partial R^2} + \frac{l_f(l_f+1)}{2\mu R^2} - E \right) + V_{fi}(\vec{R}) \right] F_{fi} = 0 . \quad (2.3)$$

The interaction potentials $V_{fi}(\vec{R})$ will be discussed in section 2.2. If the interaction potentials are isotropic, a finite set of coupled Schrödinger equations are obtained for each partial wave l , of which, only $l=0-4$ typically need to be considered for collision energies below a few mK. The coupled Schrödinger equations (Eq. 2.3) are solved subject to the following boundary conditions:

$$\begin{aligned} F_{fi}(0) &= 0 \\ F_{fi}(R) &\xrightarrow{R \rightarrow \infty} \sqrt{\frac{2\mu}{\pi \hbar^2 k_i}} \left[\frac{e^{-i(k_i R - l_i \pi/2)} \delta_{fi} - e^{i(k_i R - l_i \pi/2)} S_{fi}}{2i} \right] \end{aligned} \quad (2.4)$$

where $k_i = \sqrt{2\mu E_i/\hbar^2}$. The amplitude of the wave scattered from channel i into channel f is given by the scattering matrix element S_{fi} . All experimentally observable collision quantities can be expressed in terms of the scattering matrix. In practice, it is more convenient to work with a real-valued reaction matrix \underline{K} instead of the complex-valued \underline{S} matrix. This will be discussed in Section 3.2. The asymptotic boundary condition on F_{fi} implies that the total wave function behaves in the large R limit as:

$$\Psi_i^+ \xrightarrow{R \rightarrow \infty} \sum_f \Phi_f \left(e^{i\vec{k}_f \cdot \vec{R}} \delta_{fi} + \frac{e^{ik_f R}}{R} f_{fi}(\theta, \phi) \right) \quad (2.5)$$

Here, the scattering amplitude $f_{fi}(\theta, \phi)$ takes on the role of the scattering matrix and the exact relationship between the two quantities is derived in Section 2.1.2. In the case of identical particle scattering, the total wave function must be an eigenfunction of the nuclear permutation operator P_{12} , i.e. the wave function must be symmetrized. The boundary condition on the symmetrized wave function Ψ^+ is then given by

$$\begin{aligned} \Psi_i^+ &\xrightarrow{R \rightarrow \infty} \sum_f \Phi_f \left(\frac{e^{i\vec{k}_f \cdot \vec{R}} + e^{-i\vec{k}_f \cdot \vec{R}}}{\sqrt{2}} \delta_{fi} \right. \\ &\quad \left. + \left[\frac{f_{fi}(\theta, \phi) + f_{fi}(\pi - \theta, \pi + \phi)}{\sqrt{2}} \right] \frac{e^{ik_f R}}{R} \right) \end{aligned} \quad (2.6)$$

and the physical observables are determined by the symmetrized scattering amplitude $f_{fi}(\theta, \phi) + f_{fi}(\pi - \theta, \pi + \phi)$. The scattering amplitudes will be related to the physical quantities of interest in cold collisions (i.e., cross sections, event rates, and scattering lengths) in the next subsection.

2.1.1 Derivation of the cross section and event rate formulas

The Born approximation can be used to derive cross section and event rate formulas, in a way that brings out the structure of the scattering amplitudes and therefore makes the identical particle aspects of the scattering theory more transparent. First, consider the scattering of two non-identical spinless particles. The initial wave function in the center-of-mass coordinate system can be described by a plane wave $e^{ik_i Z}$. Here, particles a and b approach from $\theta = 0$ and $\theta = \pi$, respectively. The time-independent wave function that obeys outgoing-wave boundary conditions obeys the integral equation[25]

$$\Psi^+ = e^{ik_i Z} + \int d^3 R' G^+(R, R') V(R') \Psi^+(R') \quad (2.7)$$

where $\vec{k}_i = k \hat{Z}$ and the free particle Green function is

$$G^+(\vec{R}, \vec{R}') = -\frac{2\mu}{4\pi\hbar^2} \frac{e^{ik|\vec{R}-\vec{R}'|}}{|\vec{R}-\vec{R}'|}. \quad (2.8)$$

In the limit of large R , $|\vec{R}-\vec{R}'| \simeq R - R' \hat{R} \cdot \hat{R}'$ and the Green function becomes

$$G^+(\vec{R}, \vec{R}') \cong -\frac{2\mu}{4\pi\hbar^2} \frac{e^{ik_f R}}{R} e^{-i\vec{k}_f \cdot \vec{R}'} \quad (2.9)$$

where $\vec{k}_f \xrightarrow{R \rightarrow \infty} k \hat{R}$. Using the first Born approximation for Ψ^+ , I obtain a final expression for the scattered wave function

$$\Psi^+ \xrightarrow{R \rightarrow \infty} e^{ik_i Z} - \frac{e^{ik_f R}}{R} \frac{\mu}{2\pi\hbar^2} \int d^3 R' e^{-i\vec{k}_f \cdot \vec{R}'} V(R') e^{ik_i Z}. \quad (2.10)$$

The non-identical particle scattering amplitude $f(\theta, \phi)$ can then be extracted by comparing equation 2.5 with 2.10. The integrals in equation 2.10 will be expressed in terms of T -matrix elements in subsection 2.1.2

I turn next to the adaptation of this derivation to the case of identical particle scattering. The permutation operator P_{12} commutes with the Hamiltonian of our system and can be used to obtain new eigenfunctions with the proper symmetry. For the moment, the spin degrees of freedom will be suppressed. These will be taken into account when actually evaluating the scattering amplitude integrals (subsection 2.1.2). For the sake of clarity, I will only treat collisions between identical bosons. The new wave functions are

$$\left(\frac{1 + P_{12}}{\sqrt{2}} \right) \Psi_i = \frac{e^{ik_i Z} + e^{-ik_i Z}}{\sqrt{2}} \quad (2.11)$$

and

$$\left(\frac{1+P_{12}}{\sqrt{2}}\right)\Psi_f \xrightarrow{R\rightarrow\infty} \frac{e^{ik_f R}}{R} \frac{\mu}{2\pi\hbar^2} \times \int d^3R' \frac{e^{i\vec{k}_f\cdot\vec{R}'} + e^{-i\vec{k}_f\cdot\vec{R}'}}{\sqrt{2}} V(R') e^{ik_i Z'} . \quad (2.12)$$

Here, P_{12} acts only on the unprimed coordinates (recall $\vec{k}_f = k\hat{R}$).

Equation 2.12 still needs a little work. First, note that the integral in Eq. 2.12 is symmetric in the Z' coordinate. Adding an integral over $e^{-ik_i Z'}$ and then dividing by two, gives the following properly symmetrized expression

$$\Psi_f \xrightarrow{R\rightarrow\infty} \frac{e^{ik_f R}}{\sqrt{2}R} \frac{\mu}{2\pi\hbar^2} \times \int d^3R' \left(\frac{e^{i\vec{k}_f\cdot\vec{R}'} + e^{-i\vec{k}_f\cdot\vec{R}'}}{\sqrt{2}}\right) V(R') \left(\frac{e^{ik_i Z'} + e^{-ik_i Z'}}{\sqrt{2}}\right) . \quad (2.13)$$

Comparing Eq. 2.13 with Eq. 2.6, we find the following relationship for the symmetrized scattering amplitude

$$f(\theta, \phi) + f(\pi - \theta, \pi + \phi) = -\frac{\mu}{2\pi\hbar^2} \bar{M}_{fi} \quad (2.14)$$

where

$$\bar{M}_{fi} = \int d^3R' \left(\frac{e^{i\vec{k}_f\cdot\vec{R}'} + e^{-i\vec{k}_f\cdot\vec{R}'}}{\sqrt{2}}\right) V(R') \left(\frac{e^{ik_i Z'} + e^{-ik_i Z'}}{\sqrt{2}}\right) . \quad (2.15)$$

Mott and Massey[24] define the identical particle differential cross section as the ratio of the scattered radial flux to the incident flux in a **single** beam. The result is

$$\frac{d\sigma}{d\Omega_f} = \frac{k_f}{k_i} |f(\theta, \phi) + f(\pi - \theta, \pi + \phi)|^2 . \quad (2.16)$$

This expression for the differential cross section will be rewritten in terms of symmetrized T -matrix elements in subsection 2.1.2. The numerical solution of equation 2.3 to obtain these symmetrized T -matrix elements is the subject of chapter 3.

We are interested not only in the scattering cross section but also in the event rate for collisions. To that end, consider the scattering of two particles from a different perspective. Place the particles into a large box of dimension L on each side. The Born approximation treats scattering of particles in a box as a transition between discretized eigenstates of the box (see, for example Ref[26]). The total transition rate Γ_{fi} from eigenstate $i \rightarrow f$ is an integral of the state-to-state transition

rate W_{fi} over all distinguishable final states. The ‘‘Fermi golden rule’’ can be used to determine W_{fi} , resulting in

$$\begin{aligned}\Gamma_{fi} &= \int k_f^2 d\Omega_f dk_f \left(\frac{L}{2\pi}\right)^3 W_{fi} \\ &= \frac{2\pi}{\hbar} \int d\Omega_f k_f^2 dk_f |M_{fi}|^2 \delta(E_f - E_i) \left(\frac{L}{2\pi}\right)^3\end{aligned}\quad (2.17)$$

where $\left(\frac{L}{2\pi}\right)^3$ represents a density-of-states factor and the matrix element M_{fi} is given by

$$M_{fi} = \langle \Psi_f | V | \Psi_i \rangle = \int d^3R \left(\frac{e^{i\vec{k}_f \cdot \vec{R}} + e^{-i\vec{k}_f \cdot \vec{R}}}{\sqrt{2L^3}} \right) V(R) \left(\frac{e^{i\vec{k}_i \cdot \vec{R}} + e^{-i\vec{k}_i \cdot \vec{R}}}{\sqrt{2L^3}} \right).\quad (2.18)$$

The integral over dk_f in Eq. 2.17 is rewritten as an energy integral using $dE_f = \hbar^2 k_f dk_f / \mu$, which gives

$$\Gamma_{fi} = \frac{\mu}{4\pi^2 \hbar^4 L^3} \int d\Omega_f k_f |\bar{M}_{fi}|^2\quad (2.19)$$

where $\bar{M}_{fi} = L^3 M_{fi}$. Equation 2.19 represents the probability per second for the two particles to make a transition from state i to all final states f . The event rate constant K is defined as the transition probability per pair of particles to make the transition from state i to state f per volume per second. It is obtained by dividing Eq. 2.19 by the number of pairs per unit volume in our box $1/L^3$ and is given in terms of the scattering amplitude by

$$K_2 = \int d\Omega_f \frac{k_f}{\mu} |f(\theta, \phi) + f(\pi - \theta)|^2 = \frac{k_i}{\mu} \sigma.\quad (2.20)$$

2.1.2 Relating the scattering amplitude to the scattering matrix

The symmetrized scattering amplitude $f(\theta, \phi) + f(\pi - \theta, \pi + \theta)$ can now be expressed in terms of a corresponding symmetrized T -matrix. In general, it is necessary to include the spin degrees of freedom. I will consider the four different possibilities of scattering identical particles in distinguishable or indistinguishable initial and final spin states. The terminology ‘‘distinguishable’’ and ‘‘indistinguishable’’ is reserved for the spin degrees of freedom. Although the scattering of identical particles is considered here, an experiment can still identify these particles according to their spin state. Identical atoms in the same spin state are therefore truly indistinguishable. To simplify the presentation, consider collisions between

two spin-1 particles. The symmetrized initial plane waves are

$$\begin{aligned}\Psi_i^I &= \left(\frac{e^{ik_i Z} + e^{-ik_i Z}}{\sqrt{2}} \right) |10, 10\rangle \\ \Psi_i^D &= \frac{e^{ik_i Z} |11, 1-1\rangle + e^{-ik_i Z} |1-1, 11\rangle}{\sqrt{2}}\end{aligned}\quad (2.21)$$

and final state wave functions are

$$\begin{aligned}\Psi_f^I &= \left(\frac{e^{i\vec{k}_f \cdot \vec{R}} + e^{-i\vec{k}_f \cdot \vec{R}}}{\sqrt{2}} \right) |10, 10\rangle \\ \Psi_f^D &= \frac{e^{i\vec{k}_f \cdot \vec{R}} |11, 1-1\rangle + e^{-i\vec{k}_f \cdot \vec{R}} |1-1, 11\rangle}{\sqrt{2}}\end{aligned}\quad (2.22)$$

where the I or D superscripts indicate indistinguishable or distinguishable spin states. The spin ket notation is $|f_a m_a, f_b m_b\rangle$. The plane waves can be expanded using the following identities[27]

$$\begin{aligned}e^{ikZ} &= \sum_{l=0}^{\infty} i^l (2l+1) P_l(\cos \theta) j_l(kR) \\ e^{i\vec{k} \cdot \vec{R}} &= \sum_{l=0}^{\infty} \sum_{m=-l}^{+l} 4\pi i^l Y_{lm}^*(\theta_f, \phi_f) Y_{lm}(\theta, \phi) j_l(kR).\end{aligned}\quad (2.23)$$

Analogous expansions of the complex conjugates of the above plane waves introduce additional $(-1)^l$ factors. Inserting the plane wave expansions, the initial and final state unperturbed wave functions become

$$\begin{aligned}\Psi_i^I &= \sqrt{2} \sum_{l_i=\text{even}} i^{l_i} (2l_i+1) P_{l_i}(\cos \theta) j_{l_i}(k_i R) \chi^I \\ \Psi_i^D &= \sum_{l_i} i^{l_i} (2l_i+1) P_{l_i}(\cos \theta) j_{l_i}(k_i R) \chi^D\end{aligned}\quad (2.24)$$

and

$$\begin{aligned}\Psi_f^I &= \sqrt{2} \sum_{l_f=\text{even}} \sum_{m_f} 4\pi i^{l_f} Y_{l_f m_f}^*(\theta_f, \phi_f) Y_{l_f m_f}(\theta, \phi) j_{l_f}(k_f R) \chi^I \\ \Psi_f^D &= \sum_{l_f} \sum_{m_f} 4\pi i^{l_f} Y_{l_f m_f}^*(\theta_f, \phi_f) Y_{l_f m_f}(\theta, \phi) j_{l_f}(k_f R) \chi^D\end{aligned}\quad (2.25)$$

where $\chi^I = |10, 10\rangle$ and $\chi^D = \frac{1}{\sqrt{2}} [|11, 1-1\rangle + (-1)^l |1-1, 11\rangle]$ represent symmetrized spin basis functions. Note that the expansions for the indistinguishable

spin states are summed over **even** values of the partial wave. In the case of identical fermions scattering in indistinguishable spin states the sums would include only **odd** l 's.

The first example will be outlined in detail. The steps are the same in all cases, so I will only quote final results for the last three. For concreteness consider a spin-dependent isotropic potential $V^S(R)$;

i) indistinguishable spin state \rightarrow indistinguishable spin state

$$\begin{aligned} \bar{M}_{fi} &= \langle \Psi_f^I | V^S | \Psi_i^I \rangle = 8\pi \sum_{l_i, l_f, m_f} i^{l_f + l_i} (2l_i' + 1) Y_{l_f m_f}(\theta_f, \phi_f) \\ &\int d\Omega P_{l_i}(\cos \theta) Y_{l_f m_f}^*(\theta, \phi) \int R^2 dR j_{l_f}(k_f R) \langle \chi^I | V^S | \chi^I \rangle j_{l_i}(k_i R) . \end{aligned} \quad (2.26)$$

Using $P_l(\cos \theta) = \sqrt{\frac{4\pi}{2l+1}} Y_{l,0}$ and the orthogonality properties of the spherical harmonics, the angular integral ($\int d\Omega = 4\pi$) can be evaluated giving

$$\begin{aligned} \bar{M}_{fi} &= 8\pi \sum_{l_i = \text{even}} (2l_i + 1) P_{l_i}(\cos \theta_f) \\ &\delta_{l_i, l_f} \int R^2 dR j_{l_f}(k_f R) \langle \chi^I | V^S | \chi^I \rangle j_{l_i}(k_i R) . \end{aligned} \quad (2.27)$$

Introducing energy normalized radial wave functions[27] $\sqrt{\frac{2\mu}{\pi k}} k R j_l(kR)$, the radial integral can be related to a scattering \underline{S} - or transition \underline{T} -matrix element[27]

$$\begin{aligned} \{T\}_{fi} &= \frac{\{S\}_{fi} - \delta_{fi}}{2i} \\ &= -\pi \int dR \sqrt{\frac{2\mu}{\pi k_f}} k_f R j_{l_f}(k_f R) \langle \chi^I | V^S | \chi^I \rangle \sqrt{\frac{2\mu}{\pi k_i}} k_i R j_{l_i}(k_i R) . \end{aligned} \quad (2.28)$$

The brackets on $\{T\}_{fi}$ indicate that the matrix element is calculated in a symmetrized spin basis. The final result for the matrix element is then given by

$$\bar{M}_{fi} = -\frac{4\pi}{\mu} \frac{1}{\sqrt{k_i k_f}} \sum_{l_i = \text{even}} (2l_i + 1) P_{l_i}(\cos \theta_f) \{T\}_{fi} \quad (2.29)$$

ii) indistinguishable \rightarrow distinguishable

$$\bar{M}_{fi} = -\frac{2\sqrt{2}\pi}{\mu} \frac{1}{\sqrt{k_i k_f}} \sum_{l_i=\text{even}} (2l_i + 1) P_{l_i}(\cos \theta_f) \{T\}_{fi} \quad (2.30)$$

iii) **distinguishable** \rightarrow **indistinguishable**

$$\bar{M}_{fi} = -\frac{2\sqrt{2}\pi}{\mu} \frac{1}{\sqrt{k_i k_f}} \sum_{l_i=\text{even}} (2l_i + 1) P_{l_i}(\cos \theta_f) \{T\}_{fi} \quad (2.31)$$

iv) **distinguishable** \rightarrow **distinguishable**

$$\bar{M}_{fi} = \frac{2\pi}{\mu} \frac{1}{\sqrt{k_i k_f}} \sum_{l_i=0}^{\infty} (i)^{2l_i} (2l_i + 1) P_{l_i}(\cos \theta_f) \{T\}_{fi} \quad (2.32)$$

The last step required to obtain a total cross section or event rate constant is evaluation of the integral over final states $\int d\Omega_f$ in equations 2.16 and 2.20. In the case of distinguishable final spin states this integral is taken over **all space**. However, for indistinguishable final spin states we must restrict the integral over **half space** ($\int d\Omega_f = 2\pi$) to avoid double counting. The results for the four cases are quoted below. To derive these, one must keep in mind the caveat on the angular integration limits.

i) **indistinguishable** \rightarrow **indistinguishable**

Plugging \bar{M}_{fi} from equation 2.29 into equations 2.16 and 2.20 and using the orthogonality properties of the Legendre polynomials gives

$$\begin{aligned} \sigma &= 8\pi \sum_{l_i=\text{even}} (2l_i + 1) \frac{|\{T\}_{fi}|^2}{k_i^2} \\ K_2 &= 8\pi \sum_{l_i=\text{even}} (2l_i + 1) \frac{|\{T\}_{fi}|^2}{\mu k_i} \end{aligned} \quad (2.33)$$

This cross section expression can be checked in the s -wave limit. The scattering length is defined as $\lim_{k_i \rightarrow 0} a = (-\tan \delta/k) [24]$, where δ is the elastic phase shift. In the zero energy limit, $\{T\}_{fi} \rightarrow \delta$ and we find $\sigma = 8\pi a^2$ as expected. In practice, I calculate the scattering lengths from the \underline{S} -matrix. The diagonal \underline{S} -matrix elements are related to the phase shift [24] by $\{S\}_{ii} = e^{2i\delta_i}$. The scattering length in channel i is then given by

$$\lim_{k_i \rightarrow 0} a_i = -\frac{\ln\{S\}_{ii}}{2ik_i}. \quad (2.34)$$

ii) **indistinguishable** → **distinguishable**

$$\begin{aligned}\sigma &= 8\pi \sum_{l_i=\text{even}} (2l_i + 1) \frac{|\{T\}_{fi}|^2}{k_i^2} \\ K_2 &= 8\pi \sum_{l_i=\text{even}} (2l_i + 1) \frac{|\{T\}_{fi}|^2}{\mu k_i}\end{aligned}\quad (2.35)$$

iii) **distinguishable** → **indistinguishable**

$$\begin{aligned}\sigma &= 4\pi \sum_{l_i=\text{even}} (2l_i + 1) \frac{|\{T\}_{fi}|^2}{k_i^2} \\ K_2 &= 4\pi \sum_{l_i=\text{even}} (2l_i + 1) \frac{|\{T\}_{fi}|^2}{\mu k_i}\end{aligned}\quad (2.36)$$

iv) **distinguishable** → **distinguishable**

$$\begin{aligned}\sigma &= 4\pi \sum_{l_i=0}^{\infty} (2l_i + 1) \frac{|\{T\}_{fi}|^2}{k_i^2} \\ K_2 &= 4\pi \sum_{l_i=0}^{\infty} (2l_i + 1) \frac{|\{T\}_{fi}|^2}{\mu k_i}\end{aligned}\quad (2.37)$$

In the case of non-identical particle collisions, the cross section and event rate formulas are given by case iv) and the \underline{T} -matrix element is calculated in an unsymmetrized spin basis.

There is one more identical particle detail that must be considered. The event rate K_2 describes the rate at which **pairs** of atoms collide, whereby K_2 inelastic events will generally lead to $2K_2$ atoms lost in unit trap volume per unit time. Generally, the most useful parameter is the **atom-loss** rate constant, the coefficient of the density squared in the rate equation. This quantity is $L_2 = K_2/(1 + \delta)$. The denominator $(1 + \delta)$ is needed because the number of pairs depends on the initial spin state. If the initial spin states are the same $\delta = 1$, otherwise $\delta = 0$. For example, a gas of N identical atoms initially in indistinguishable spin states will have $N(N - 1)/2$ pairs as opposed to the distinguishable case which will have $N_a N_b$ pairs. However, these additional factors of two are easily accommodated since K_2 in equations 2.33 and 2.35 is a factor of two larger than in equations 2.36 and 2.37.

The definition for the atom loss rate constant will therefore be taken as

$$(L_2)_{fi} \equiv 4\pi (2l_i + 1) \frac{|\{T\}_{fi}|^2}{\mu k_i} . \quad (2.38)$$

The rate equation controlling the number of α spin state atoms would thus read:

$$\frac{dn_\alpha}{dt} = \sum_\beta \sum_{\{\gamma\delta\}} (1 + \delta_{\alpha,\beta}) [L_2(\gamma\delta \rightarrow \alpha\beta) n_\gamma n_\delta - L_2(\alpha\beta \rightarrow \gamma\delta) n_\alpha n_\beta] \quad (2.39)$$

where n_α is the density of atoms in the α spin state. There is some confusion in the literature regarding this terminology. Generally, the published results that were termed ‘‘event rate constants’’, e.g. in Ref.[28], are understood to be the coefficient of the density squared in the rate equations, (i.e., what we call the atom-loss rate). However, our definition of L_2 used in the above rate equation agrees with the ‘‘standard’’ definition of K_2 .

The last situation that needs to be examined is the case of an anisotropic spin-dependent potential $V^S(R, \Omega)$. Returning to the first indistinguishable spin isotropic example (case i), equation 2.26 can be generalized as follows

$$\begin{aligned} \bar{M}_{fi} &= 8\pi \sum_{l_i, l_f, m_f} i^{l_i+l_f} (2l_i + 1) Y_{l_f m_f}(\theta_f, \phi_f) \\ &\quad \sqrt{\frac{4\pi}{2l_i + 1}} \int R^2 dR j_{l_f}(k_f R) \langle \chi^I Y_{l_f m_f}(\Omega) | V^S | Y_{l_i 0}(\Omega) \chi^I \rangle j_{l_i}(k_i R) . \end{aligned} \quad (2.40)$$

The new expressions for the perturbative \underline{S} - and \underline{T} -matrix elements are

$$\begin{aligned} \{T\}_{fi}^{l_f m_f l_i} &= \frac{\{S\}_{fi}^{l_f m_f l_i} - \delta_{fi}}{2i} \\ &= -\pi \int dR \sqrt{\frac{2\mu}{\pi k_f}} k_f R j_{l_f}(k_f R) \\ &\quad \langle \chi^I Y_{l_f m_f}(\Omega) | V^S | Y_{l_i 0}(\Omega) \chi^I \rangle \sqrt{\frac{2\mu}{\pi k_i}} k_i R j_{l_i}(k_i R) \end{aligned} \quad (2.41)$$

which can be substituted back into the equation above to give

$$\bar{M}_{fi} = -\frac{4\pi}{\mu} \frac{4\pi}{\sqrt{k_i k_f}} \left| \sum_{l_f=\text{even}} \sum_{m_f} \sum_{l_i=\text{even}} \sqrt{2l_i + 1} Y_{l_f m_f}(\Omega_f) \{T\}_{fi}^{l_f m_f l_i} \right| . \quad (2.42)$$

The matrix element \bar{M}_{fi} for cases ii) and iii) will again be a $\sqrt{2}$ smaller than the one given in Eq. 2.42 and case iv) a factor of two smaller. The cross sections and

event rates are obtained in the same fashion, although one should keep in mind the caveats on the $d\Omega_f$ integration limits. The final results for the anisotropic potential can be summarized as follows

$$\sigma = 4\pi \left| \sum_{l_f m_f l_i} \sqrt{2l_i + 1} \frac{\{T\}^{l_f m_f l_i}}{k_i} \right|^2 (1 + \delta) \quad (2.43)$$

and

$$L_2 = \frac{4\pi}{\mu k_i} n \left| \sum_{l_f m_f l_i} \sqrt{2l_i + 1} \{T\}^{l_f m_f l_i} \right|^2. \quad (2.44)$$

An anisotropic potential couples the different partial waves and therefore these must be added coherently (with the appropriate limits on the sum over the initial and final partial waves). Finally, the δ function in Eq. 2.43 is one if the two atoms are initially in the same spin state and zero if the two atoms are initially in distinguishable spin states.

2.2 Interaction potentials

The complete description of two interacting multi-component atoms is extremely complex. Levy and co-workers[29, 30] have identified a fourteen term Hamiltonian valid for diatomic molecules in the Born-Oppenheimer limit[31]. However, most of these interactions are vanishingly small for two ground state alkali atoms. In fact, most of the interesting cold collision physics comes about simply because the collision energies are much smaller than the atomic hyperfine splittings. Consequently the collision partners can in some cases resonate (i.e. at a Feshbach resonance in asymptotically closed channels). Moreover, if the partners change hyperfine states, enough energy can be liberated to eject the atoms from the trap. Or if the trap is magnetic, the collision can produce untrapped hyperfine states and again the atoms are lost. These hyperfine changing collisions are generally termed spin-exchange collisions, although one should keep in mind that other interactions besides electronic spin-exchange can also change the hyperfine states. True spin-exchange collisions can be viewed as resulting from a transformation between angular momentum coupling schemes. At small internuclear separations R , the two electronic spins tend to lock and precess around the total angular momentum vector. At large R the electrostatic exchange splitting decays exponentially and the electron spin on each atom now prefers to couple to the corresponding nuclear spin, precessing around the total atomic angular momentum vector of each atom. However as the atoms recede, the small R evolution of the total electronic spin states will not in general allow the spins to recouple in exactly the same hyperfine states

that initially approached. Spin-exchange coupling is generally strong, leads to large trap loss rates, and is something to be avoided. This can be arranged either through the choice of symmetry (e.g., by trapping doubly polarized spin states, also known as “stretched states”) or else through energetic considerations. A second and much weaker loss process frequently occurs via the magnetic dipole-dipole interaction between the two valence electrons. It can usually be neglected unless one needs the loss rate from a spin-exchange forbidden collision.

Complete descriptions of these interactions are provided in this section. Subsection 2.2.1 describes the construction of the Born-Oppenheimer potentials. The hyperfine Hamiltonian is presented in subsection 2.2.2 and the magnetic dipole-dipole Hamiltonian in subsection 2.2.3. Finally, magnetic field induced Feshbach resonances will be discussed in subsection 2.2.4.

2.2.1 Constructing the Born-Oppenheimer potentials

The motion of the constituent charged particles of the diatom is controlled by two very different time scales. The electrons are much lighter than the nuclei and therefore move at greater velocities. The Hamiltonian describing the complete system, $H = H_N + H_e$, can be approximately separated into a nuclear and electronic component. This is known as the Born-Oppenheimer limit[31]. The Born-Oppenheimer potential curves are constructed by freezing the interatomic separation at a given value R , and then evaluating the energies of the resulting electronic eigenstates of H_e . These energies vary with R and constitute a set of potential energy curves. The physics underlying these potentials is qualitatively different in regions of small and large internuclear separations. The division between these two regions is determined by the overlap of the atomic electronic clouds, which begins to become exponentially small beyond $R \sim 20$ a.u. in the alkalis. Information regarding these two regions is generally collected from different sources and must then be smoothly connected through the transition region near $R \sim 20$ a.u.

The small R region is characterized by large overlaps of the electronic clouds; here one must use molecular concepts to correctly describe the interaction of the collision pair. In the case of alkali atom ground state collisions, the potential energy depends solely on the internuclear separation R and the orientation of the two atom’s valence electronic spins ($s_i=1/2$) which couple into singlet ($S=0$), where ($\vec{S} = \vec{s}_a + \vec{s}_b$) or triplet ($S=1$) configurations. The Hund’s case (a) designations for these states are $X^1\Sigma_g^+$ and $a^3\Sigma_u^+$ for the singlet and triplet respectively. The spin dependence of the potential energy is a consequence of the Pauli exclusion principle which requires the wave function to have an odd permutation symmetry under exchange of electrons[32]. As one can imagine, **ab initio** calculations to determine the interactions of multi-electron alkali atoms require sophisticated numerical techniques[33]. Fortunately, molecular spectroscopists have devoted a great deal of attention to measuring ro-vibrational spectra. In turn, these spectra can be

inverted to determine a corresponding potential using standard techniques such as RKR[34] or inverted perturbation analysis (IPA)[35]. References for the small R Born-Oppenheimer potentials used in this work are given in Table 2.1.

The physics simplifies as the overlap of the electron clouds decreases. The residual overlap leads to a long range exchange term of the form $V^{\text{ex}} = \pm AR^\alpha \exp^{-\beta R}$ where $+$ is used for the triplet state and $-$ for the singlet. Analytical values for α and β are derived in Ref.[36]. These expressions are given in terms of the valence electron binding energy E_b , which for identical atoms becomes $\alpha = \frac{7}{2\sqrt{2E_b}} - 1$ and $\beta = 2\alpha$. The value of the overall scaling coefficient A is determined from the difference $V_{S=1} - V_{S=0}$ near the transition $R \sim 20$ a.u., (see for example Ref[37]). The remaining large R electrostatic interactions are a result of ‘‘instantaneous’’ multipole moments. The motion of the electrons leads to small fluctuations in the charge density surrounding each atom. In turn, one atom can polarize the other setting up an momentary dipole moment which then attracts the first. This is the van der Waals or dispersion force. In the case of two alkali atoms colliding in their atomic ground states, the dispersion potential is given by $V^d = -C_6/R^6 - C_8/R^8 - C_{10}/R^{10}$. **Ab initio** calculations[38, 39, 40] for the dispersion coefficients C_n have proven reliable to within a few %. Ref.[38] is used for the C_8 and C_{10} coefficients. C_6 coefficients are taken from a variety of sources which are listed in Table 2.1. The dispersion potentials will also be modified by retardation effects. However, current experiments have not been able to separate ground state retardation effects from uncertainties associated with other interactions. Retardation effects are therefore neglected. (Retardation effects have been observed in pseudo-bound excited state measurements, see for example Ref.[21]). The Rb Born-Oppenheimer potentials used in this work are shown in Fig. 2.1.

Table 2.1: Sources of information for constructing the Born-Oppenheimer potentials. The singlet and triplet columns list the method used in the corresponding reference to obtain the small R part of the potential. The C_6 coefficients are the nominal values used in this work and are cited along with the corresponding reference.

Atom	Singlet	Triplet	C_6
Li	RKR[41]	RKR[41]	1393.4[42]
Na	RKR[43]	RKR[43]	1538.9[44]
K	IPA[45]	RKR[46]	3897.0[39]
Rb	IPA[47]	ab initio [33]	4700.0[17]
Cs	IPA[48]	ab initio [33]	6851.0[39]

The potentials as given are still not accurate enough for ultracold collision calculations. Typically, the highest bound state measured with conventional molecular spectroscopy is more than 2 cm^{-1} below the dissociation threshold. Ex-

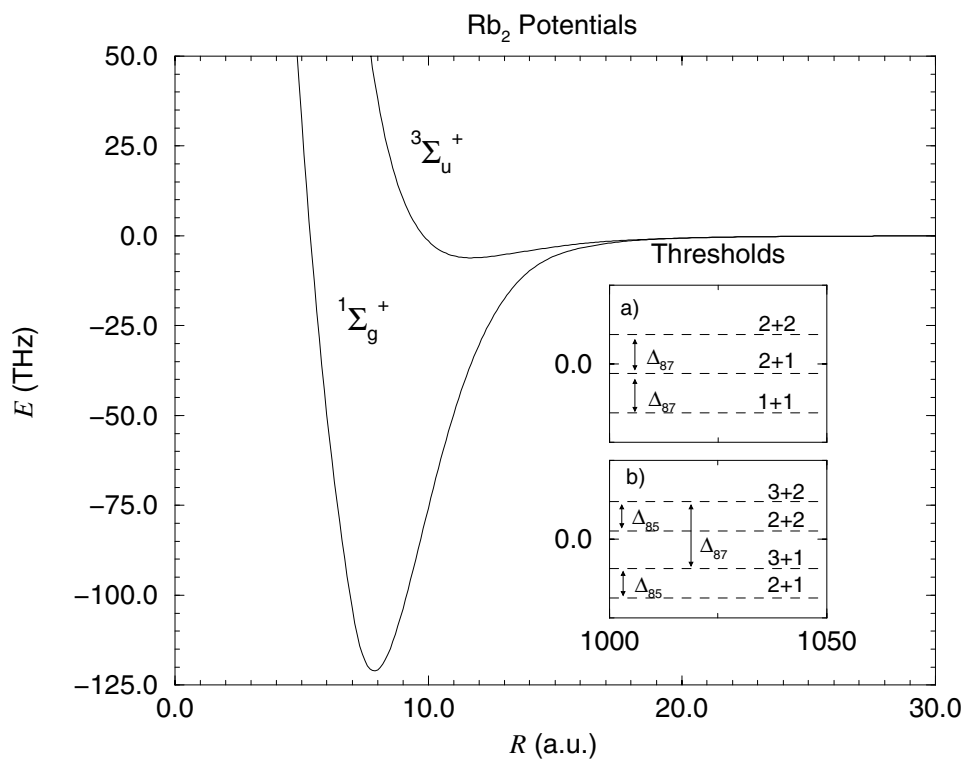


Figure 2.1: Singlet and triplet Rb₂ Born-Oppenheimer potentials. Hyperfine split thresholds are indicated in the inset for a) two ⁸⁷Rb atoms and b) ⁸⁷Rb + ⁸⁵Rb collision. The atomic hyperfine quantum numbers $f_a + f_b$ are indicated at each threshold. The values of the energy splittings are $\Delta_{87} = 6.835$ GHz and $\Delta_{85} = 3.036$ GHz

trapolating the Born-Oppenheimer potentials beyond this point has proven unreliable. In order to obtain collision parameters which agree with experiment we add a correction to the inner wall of the singlet and triplet potentials of the form[49]

$$\Delta V(R) = \begin{cases} C_S \tan^{-1} \left[\left(\frac{R-R_e}{\Delta R} \right)^2 \right], & R < R_e \\ 0, & R > R_e \end{cases} \quad (2.45)$$

where R_e denotes the minimum of the well and ΔR is a width parameter generally taken to be 2 Bohr. The energy dependence of the phase shifts has been tested using other functional forms for the correction, such as quadratic, cubic, and quartic polynomials in R , all of which give nearly identical results.

2.2.2 Atomic hyperfine Hamiltonian

The atomic hyperfine Hamiltonian represents the coupling of an electron with the electromagnetic field created by the charged nucleus. In general, for nuclei with spin $i > 1/2$ the Hamiltonian is quite complicated. For example, electric and magnetic multipole terms of order $k \leq 2i$ are allowed[50]. However, expectation values of these multipole terms average to zero for spherically symmetric atoms ($L=0$) which will be the case for alkali atoms in their ground state. The lone remaining term, commonly referred to as Fermi's "contact term", is a result of the non-zero spatial extent of the nucleus and can be expressed as[51]

$$H^{\text{ahf}} = \frac{-8\pi}{3} |\Psi_e(0)|^2 \langle \vec{\mu}_e \cdot \vec{\mu}_n \rangle \quad (2.46)$$

where $\vec{\mu}_e$ and $\vec{\mu}_n$ are the magnetic moments of the electron and nucleus, respectively. Evaluation of H in this representation is complicated by the existence of the electronic wave function term $|\Psi_e(0)|^2$. We can avoid this problem by introducing measured hyperfine splitting energies. (The review paper by Arimondo, **et al.**[52] is an excellent resource for this information.) H can be rewritten in the following form

$$H^{\text{ahf}} = C(\vec{f}_a^2 - \vec{s}_a^2 - \vec{i}_a^2) \quad (2.47)$$

where $\vec{f}_a = \vec{s}_a + \vec{i}_a$ and C is a constant which can be related to the hyperfine splitting Δ . H^{ahf} is diagonal in the basis $|f_a(s_a i_a) m_{f_a}\rangle$. Requiring the barycenter of the alkali hyperfine Hamiltonian to be $E=0$, C is given by

$$C = \Lambda \frac{\Delta}{2i + 1}. \quad (2.48)$$

Here, $\Lambda = +1$ if the nuclear magnetic moment $\vec{\mu}_n$ is positive or $\Lambda = -1$ if it is negative. The sign determines whether the hyperfine structure is "standard" (i.e.,

$E(f = i + s) > E(f = i - s)$ or “inverted” ($E(f = i + s) < E(f = i - s)$). The total hyperfine Hamiltonian H^{hf} for the collision complex taken to be simply the sum of the two atomic hyperfine Hamiltonians H^{ahf}

$$H^{\text{hf}} = \Lambda_a \frac{\Delta_a}{2i_a + 1} (\vec{f}_a^2 - \vec{s}_a^2 - \vec{i}_a^2) + \Lambda_b \frac{\Delta_b}{2i_b + 1} (\vec{f}_b^2 - \vec{s}_b^2 - \vec{i}_b^2). \quad (2.49)$$

The hyperfine split thresholds for both homonuclear and heteronuclear Rb collisions are shown in the inset of Fig. 2.1. The intra-atomic hyperfine Hamiltonian as well as any R -dependence in H^{hf} are neglected.

2.2.3 Magnetic dipole interaction

The magnetic dipole Hamiltonian can be constructed by treating the interaction of a magnetic dipole (i.e., valence electron a) with the field created by a second dipole (valence electron b). Starting with the classical expression for this interaction[51] and substituting quantum mechanical expressions for the electronic moments leads to the following relationship (in a.u.)

$$H^{\text{ss}} = -\vec{\mu} \cdot B(\vec{r}) = -\alpha^2 \left(\frac{3(\hat{n} \cdot \vec{s}_a)(\hat{n} \cdot \vec{s}_b) - \vec{s}_a \cdot \vec{s}_b}{R_{ee}^3} \right) \quad (2.50)$$

where α is the fine structure constant. The vector \vec{r} is drawn from dipole a to dipole b and is defined as $R_{ee}\hat{n}$. For our purposes, R_{ee} can be approximated as the internuclear separation R . We do not need to include the s -wave contact term (which is important for the hyperfine interaction) because the two electrons repel each other. Therefore, the electron pair wave function is exponentially small in the limit $R_{ee} \rightarrow 0$. H^{ss} is most conveniently evaluated in the molecular frame with \hat{n} defining the spin quantization axis. In the spin representation $|S\Sigma\rangle$, the Hamiltonian is diagonal, with matrix elements given by[53]

$$V_{S\Sigma} = -\frac{\alpha^2}{2R^3} (3\Sigma^2 - S(S+1)) . \quad (2.51)$$

Here, $\Sigma = \Sigma_a + \Sigma_b$ represents the total projection of the electronic spin onto the internuclear axis.

The effect of the magnetic dipole term in the molecular frame is to lift the spin projection degeneracy of the triplet state. This behavior is mimicked by an additional effect known as the second-order spin-orbit interaction[53, 29, 54]. The second-order spin-orbit interaction becomes important when the electronic clouds overlap such that indirect perturbative coupling to excited electronic molecular states can modify the direct spin-spin interaction. For ground state alkali collisions, only the $\sum_i (L_i^+ s_i^- + L_i^- s_i^+)/2$ part of the single electron spin-orbit Hamiltonian[53, 54] contributes to the interaction. Here, $L^+ S^-$ are the standard raising and lowering op-

erators for the i th electrons orbital angular momentum and spin, respectively. Mies, **et al.**[54] have shown that the dominant interactions come from coupling the triplet Born-Oppenheimer $^3\Sigma_u$ state with nearby excited $(2S+1)\Pi_u$ states. The interaction is short-ranged and its strength scales with Z . The inclusion of this term is important only for the heavier atoms such as Rb and Cs. Analytical expressions for Rb and Cs have been derived in Ref[54].

Before moving on, it is instructive to examine the operator structure of H^{ss} in the lab frame. Derivations are given in Refs.[29, 50] and accordingly only the final result is given here

$$H^{\text{ss}} = -\frac{\sqrt{6}\alpha^2}{R^3} \left[\sum_q (-1)^q C_q^2 (s_a^1 \otimes s_b^1)_{-q}^2 \right]. \quad (2.52)$$

$(s_a^1 \otimes s_b^1)_{-q}^2$ represents the contraction of two first-rank spin tensors into a second-rank tensor. The important result for cold collisions is the introduction of an angular dependence through the term $C_q^2 = \sqrt{\frac{4\pi}{5}} Y_{2q}(\theta, \phi)$. The second-rank nature of the spherical harmonic implies that incident s -waves will couple only with d -wave exit channels. However, the H^{ss} operator is an overall scalar and thus is rotationally invariant. Therefore, the squared total angular momentum \vec{F}^2 ($\vec{F} = \vec{f} + \vec{l}$) still commutes with the zero-field Hamiltonian.

2.2.4 External magnetic field and Feshbach resonances

The cold collisions community has energetically studied the possibility of influencing cold collisions with external fields. In principle this would allow condensate properties to be tailored. Although several methods have been proposed[55, 56, 14] probably the simplest and most robust approach is to induce a Feshbach resonance in the collision of two atoms by applying a static magnetic field. The scattering length can be varied between $\pm\infty$ as the external magnetic field is swept through the resonance field value, as has been demonstrated experimentally now, in Na condensates[15] and in thermal Rb[16, 17] and Cs[18] clouds.

The physics is rather straightforward. First, the magnetic field Hamiltonian is

$$H^{\text{B}} = -B [g\mu_e(s_z^{\text{a}} + s_z^{\text{b}}) + \mu_{\text{N}}(g_{\text{N}}^{\text{a}} i_z^{\text{a}} + g_{\text{N}}^{\text{b}} i_z^{\text{b}})] . \quad (2.53)$$

The magnetic field $\vec{B} = B\hat{z}$ is assumed to be constant and in the direction \hat{z} that defines the spin quantization axis. The constants $g\mu_e$ and $g_{\text{N}}\mu_{\text{N}}$ include the gyromagnetic ratio g and magneton $\mu_e = -e\hbar/2m_e$ for the electron and $\mu_{\text{N}} = e\hbar/2m_{\text{P}}$ for the nucleus. The individual atom spins are again labeled by a and b. The effect of Eq. 2.53 is two-fold: first the spin projection degeneracy is lifted which shifts and splits the final state thresholds; second, the magnetic field couples the

entrance channel to additional spin configurations. H^B conserves the total angular momentum projection m_F but not its squared magnitude \vec{F}^2 . ^{85}Rb atomic hyperfine thresholds and the thresholds for a $|2, -2\rangle_{85} + |2, -2\rangle_{85}$ collision complex are shown as a function of magnetic field in Fig. 2.2. (The notation $|f, m_f\rangle_A$ will be used throughout to define the isotope (A) and hyperfine spin state of each colliding atom.) A Feshbach resonance occurs when the collision energy becomes sufficiently close to the energy of a quasi-bound state associated with a closed channel that is coupled to the entrance channel. As a first approximation, one can consider these quasi-bound states as being “attached” to a particular threshold which are then shifted by the magnetic field. A schematic of a magnetic field induced Feshbach resonance is shown in Fig. 2.3. Two situations can occur. A bound state can either be added or removed from the potentials; either case results in a change of the phase shift by π radians as a function of B . A scattering length that approaches $-\infty$ as B increases toward the resonance value B_R (from low-field) indicates that the resonance came “down” out of the continuum (i.e., an additional bound state is added for $B > B_R$). This is the general scenario for magnetically trapped atoms as observed in Ref.[16, 17, 15]. The entrance channel threshold rises with increasing field, which is why they are called “weak-field-seeking” (see Fig. 2.3). Strong-field-seeking states can be trapped with optical methods; their threshold energies decrease with increasing field strength, and the most likely scenario is therefore a bound state that pops above the entrance threshold at $B > B_R$. In this instance, the scattering length $a \rightarrow +\infty$ as B approaches B_R from below. This was observed for Na[15] and Cs[18] collisions. The scattering length behavior near the resonance for both situations is shown in Fig. 2.4. The scattering length near a Feshbach resonance is often parameterized with the following expression[15]

$$a = a_0 \left(1 - \frac{\Delta}{B - B_R} \right) \quad (2.54)$$

where Δ is the width of the resonance and a_0 is the zero-field value of the scattering length.

2.3 Angular momentum representations

Different angular momentum coupling schemes play a key role in different aspects of the collision physics. In this section, I will define the different coupling schemes and outline the advantages of each. Subsection 2.3.1 discusses the symmetrization of each representation and presents the corresponding identical particle selection rules. Subsection 2.3.2 presents the unitary transformation matrix elements to transform back and forth from the short range representation to the various asymptotic representations.

Any collision event begins with atoms trapped in their individual atomic

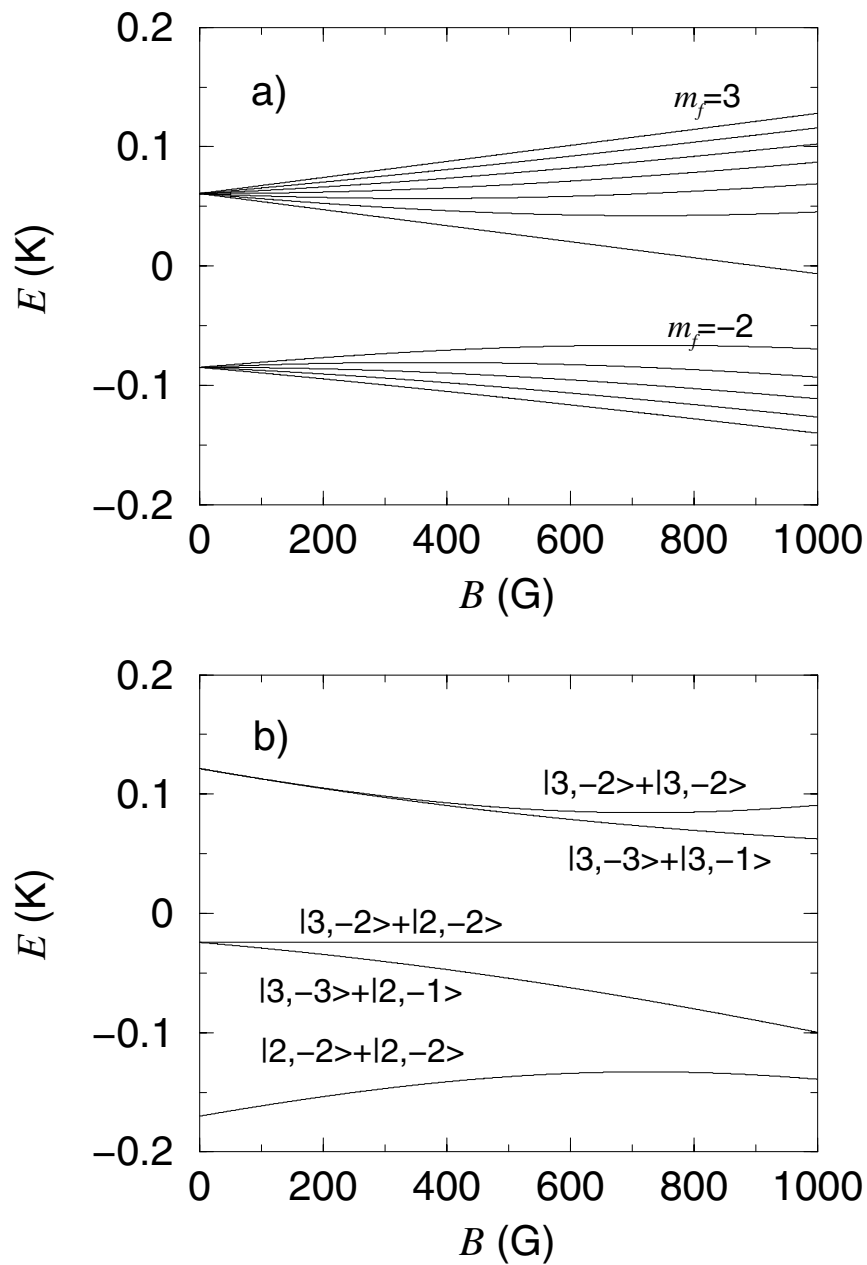


Figure 2.2: a) ^{85}Rb atomic thresholds versus magnetic field. The projection of f_a is labeled for the highest energy state in each hyperfine manifold.

b) Thresholds versus magnetic field for a collision of two $|2, -2\rangle_{85}$ atoms. The channel labels are given in terms of the atomic hyperfine quantum numbers $|f_a m_{f_a}\rangle + |f_b m_{f_b}\rangle$.

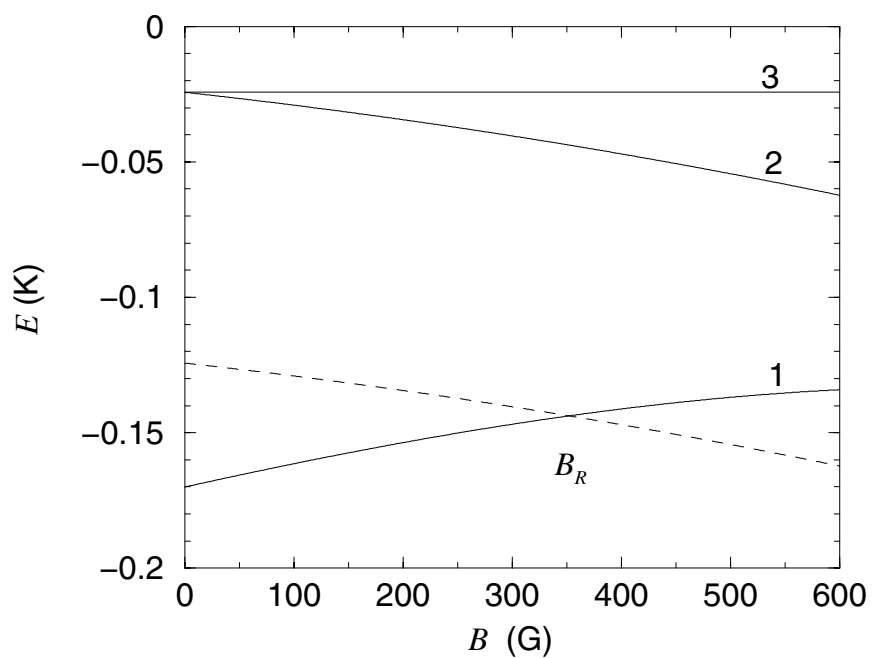


Figure 2.3: Schematic of a Feshbach resonance. The resonance state (dashed lines) is attached to threshold 2. The collision energy is relative to threshold 1 and becomes degenerate with the resonance state energy at the field value labeled B_R . In this example, the scattering length would approach $-\infty$ as B is increased to B_R .

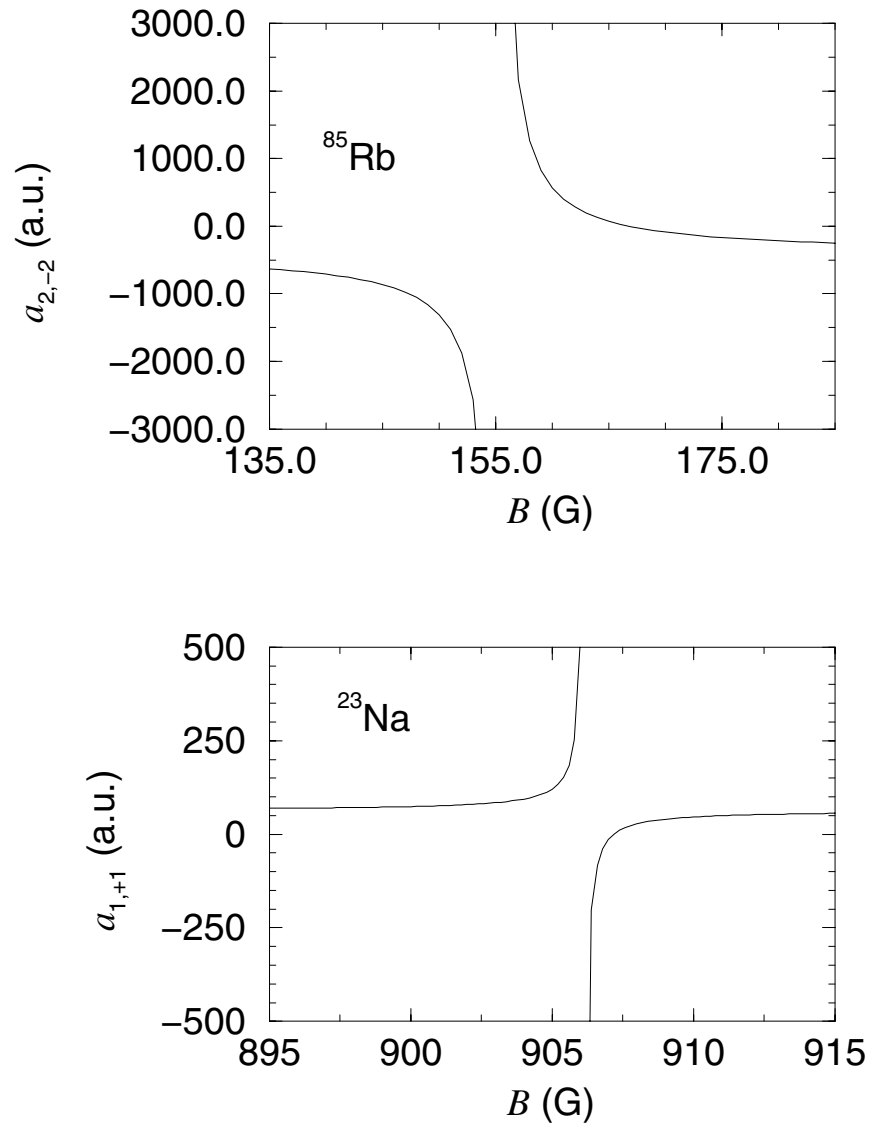


Figure 2.4: Scattering length versus magnetic field in the presence of a Feshbach resonance.

a) Feshbach resonance observed[17] in the collision of two ^{85}Rb $|2, -2\rangle$ atoms. The scattering length behavior on resonance indicates a bound state is added to the potentials.

b) Feshbach resonance observed[15] in the collision of two ^{23}Na $|1, +1\rangle$ atoms. The scattering length behavior on resonance indicates a bound state is removed from the potentials.

hyperfine state $\vec{f}_i = \vec{s}_i + \vec{i}_i$ ($i \equiv \{a, b\}$). This provides the first natural choice for an angular momentum representation and I will refer to it as the

$$\text{uncoupled hyperfine representation} \equiv |f_a m_{f_a}, f_b m_{f_b}, l m_l\rangle .$$

Here, l represents the nuclear rotation (or partial wave) and m_α the projection of the α angular momentum vector on a space-fixed quantization axis. The collision dynamics are simpler in a coupled representation. In the absence of a magnetic field (and when dipolar relaxation can be neglected), both l^2 and f^2 (where $\vec{f} = \vec{f}_a + \vec{f}_b$) are conserved quantities. The coupled Schrödinger equations therefore have a block diagonal structure in the

$$\text{coupled hyperfine representation} \equiv |(f_a f_b) f m_f, l m_l\rangle .$$

This representation is still useful in the presence of a magnetic field that is a sufficiently small perturbation. If the dipole interaction is included in the Hamiltonian, the

$$\text{total angular momentum representation} \equiv |(f l) F m_F\rangle$$

is a better basis, because in the absence of a magnetic field the Hamiltonian is again block diagonal.

The Hamiltonian expressed in any of the three representations discussed so far becomes diagonal as $R \rightarrow \infty$ (again neglecting magnetic field). In the presence of a magnetic field, the asymptotic Hamiltonian $H(R \rightarrow \infty) = H^{\text{hf}} + H^B$ is diagonalized. The resulting eigenvectors \underline{U} are used to transform the complete potential matrix $\underline{U}^T \underline{V}(R) \underline{U}$ into this eigenchannel representation. The eigenvalues provide the channel thresholds. For the field strengths I will consider, the eigenchannel representation is very nearly the uncoupled hyperfine representation and will be referred to as such. These representations are the most suitable for solving the coupled Schrödinger scattering equations since the asymptotic boundary conditions can be easily applied. However, at small R the dominant interaction is provided by the Born-Oppenheimer molecular potentials. These are diagonal in a total electronic spin basis ($\vec{S} = \vec{s}_a + \vec{s}_b$) which I will refer to as the

$$\text{short range representation} \equiv |S m_S, I m_I, l m_l\rangle .$$

To help identify nuclear permutation symmetry, the nuclear spins are also coupled to form a resultant $\vec{I} = \vec{i}_a + \vec{i}_b$. The short range representation can also be written in terms of total spin $\vec{f} = \vec{S} + \vec{I}$, but generally what controls most of the coupled-channel dynamics is the projection of the hyperfine states onto the singlet and triplet Born-Oppenheimer states.

2.3.1 Symmetries

Collisions of identical particles are of paramount interest and as such we must consider the symmetrization of the total wave function in accord with the Pauli principle. The radial piece of the total wave function (Eq. 2.2) is automatically symmetric since it depends only on the magnitude of R . We therefore need only to consider the effect of the symmetrization operator $(1 + (-1)^p P_{12})$ on the angular momentum representations presented in the previous section. The $(-1)^p$ phase is included to handle both bosonic ($p = 0$) and fermionic ($p = 1$) symmetries. In the center-of-mass representation, the spatial part of P_{12} is equivalent to the parity operator, which applied to the nuclear rotation part of the wave function ($|lm_l\rangle = Y_{lm}(\theta, \phi)$) yields

$$P_{12}|lm_l\rangle = (-1)^l|lm_l\rangle . \quad (2.55)$$

The symmetrization of the uncoupled hyperfine representation is therefore straightforward

$$(1 + (-1)^p P_{12})|f_a m_{f_a}, f_b m_{f_b}, lm_l\rangle = |f_a m_{f_a}, f_b m_{f_b}, lm_l\rangle + (-1)^{p+l}|f_b m_{f_b}, f_a m_{f_a}, lm_l\rangle . \quad (2.56)$$

Note that this relationship immediately implies that collisions of identical atoms in the same hyperfine state (i.e., indistinguishable spin states) are allowed only for even partial waves for bosons and odd partial waves for fermions. The symmetry of the coupled hyperfine representation can be obtained by first decomposing it into the uncoupled representation and applying P_{12}

$$(1 + (-1)^p P_{12})|(f_a f_b) f m_f, lm_l\rangle = (1 + (-1)^p P_{12}) \sum_{m_{f_a}, m_{f_b}} \langle f_a m_{f_a}, f_b m_{f_b} | f m_f \rangle |f_a m_{f_a}, f_b m_{f_b}, lm_l\rangle \quad (2.57)$$

Using the Clebsch-Gordan identity[57]

$$\langle f_a m_{f_a}, f_b m_{f_b} | f m_f \rangle = (-1)^{f_a+f_b-f} \langle f_b m_{f_b}, f_a m_{f_a} | f m_f \rangle \quad (2.58)$$

and recoupling the hyperfine momenta gives our final expression

$$(1 + (-1)^p P_{12})|(f_a f_b) f m_f, lm_l\rangle = |(f_a f_b) f m_f, lm_l\rangle + (-1)^{f_a+f_b-f+l+p}|(f_b f_a) f m_f, lm_l\rangle . \quad (2.59)$$

In the case $f_a = f_b$ definite selection rules are obtained in terms of f and l . A similar procedure can be used for the short range representation and one finds

$$(1 + (-1)^p P_{12}) |(s_a s_b) S m_s, (i_a i_b) I m_I, l m_l\rangle = \quad (2.60)$$

$$|(s_a s_b) S m_s, (i_a i_b) I m_I, l m_l\rangle$$

$$+ (-1)^{s_a + s_b - S + i_a + i_b - I + l + p} |(s_b s_a) S m_s, (i_b i_a) I m_I, l m_l\rangle .$$

The phase factor can be simplified by considering the case of identical alkali atoms ($s_i = 1/2, i_a = i_b$) and noting that $\sum_i (s_i + i_i + p)$ will always be even. In this case, the short range representation is manifestly symmetric with states allowed only when the phase factor $(-1)^{S+I+l}$ is equal to +1. Finally, the symmetry of the total angular momentum representation is given by the symmetry of its components

$$(1 + (-1)^p P_{12}) |((f_a f_b) f l) F m_F\rangle = |((f_a f_b) f l) F m_F\rangle + \quad (2.61)$$

$$(-1)^{f_a + f_b - f + l + p} |((f_b f_a) f l) F m_F\rangle .$$

2.3.2 Transformations

The four representations presented in the last section are connected by unitary transformations. Transformations between the different asymptotic hyperfine basis require one or at most two recoupling steps. However, connecting the short range representation with the various asymptotic representations requires a little more effort. The derivations are not tricky, as they require only standard angular momentum algebra techniques and consequently, only the results will be quoted here.

i) uncoupled hyperfine representation \leftrightarrow short range representation

$$\{\langle S m_s I m_I l' m_{l'} | f_a m_{f_a} f_b m_{f_b} l m_l \rangle\} = \quad (2.62)$$

$$\delta_{l,l'} \delta_{m_l, m_{l'}} \sum_{f, m_f} \langle S m_s, I m_I | f m_f \rangle \langle f_a m_{f_a} f_b m_{f_b} | f m_f \rangle$$

$$\sqrt{(2f_a + 1)(2f_b + 1)(2S + 1)(2I + 1)}$$

$$\begin{pmatrix} s_a & i_a & f_a \\ s_b & i_b & f_b \\ S & I & f \end{pmatrix} \left(\frac{1 + (1 - \delta_{f_a, f_b})(-1)^{S+I+l}}{\sqrt{2 - \delta_{f_a, f_b}}} \right) .$$

The $\{\}$ brackets again indicate that this is a symmetrized matrix element and $\begin{pmatrix} \vdots \\ \vdots \\ \vdots \end{pmatrix}$ represents a 9-J symbol.

ii) coupled hyperfine representation \leftrightarrow short range representation

$$\begin{aligned}
\{\langle Sm_s Im_I l' m_{l'} | (f_a f_b) f m_f l m_l \rangle\} &= \delta_{l,l'} \delta_{m_l, m_{l'}} \langle Sm_s, Im_I | f m_f \rangle \\
&\sqrt{(2f_a + 1)(2f_b + 1)(2S + 1)(2I + 1)} \\
\begin{pmatrix} s_a & i_a & f_a \\ s_b & i_b & f_b \\ S & I & f \end{pmatrix} &\left(\frac{1 + (1 - \delta_{f_a, f_b})(-1)^{S+I+l}}{\sqrt{2 - \delta_{f_a, f_b}}} \right). \tag{2.63}
\end{aligned}$$

iii) total angular momentum representation \leftrightarrow short range representation

$$\begin{aligned}
\{\langle Sm_s Im_I l' m_{l'} | (fl) F m_F \rangle\} &= \delta_{l,l'} \delta_{m_l, m_{l'}} \sum_{m_f, m_l} \tag{2.64} \\
&\langle Sm_s, Im_I | f m_f \rangle \langle f m_f l m_l | F m_F \rangle \\
&\sqrt{(2f_a + 1)(2f_b + 1)(2S + 1)(2I + 1)} \\
&\begin{pmatrix} s_a & i_a & f_a \\ s_b & i_b & f_b \\ S & I & f \end{pmatrix} \left(\frac{1 + (1 - \delta_{f_a, f_b})(-1)^{S+I+l}}{\sqrt{2 - \delta_{f_a, f_b}}} \right).
\end{aligned}$$

The unsymmetrized versions of these transformations are obtained by simply neglecting the $(1 + (1 - \delta_{f_a, f_b})(-1)^{S+I+l})/\sqrt{2 - \delta_{f_a, f_b}}$ term in each equation.